Optical Architectures for Signal Processing - Part A

B. Cabon
IMEP, UMR 5130 INPG-UJF-CNRS
B.P.257 38016 Grenoble Cedex
France

SUMMARY:

The progress achieved in performing optoelectronic components makes feasible the generation of microwave functions using all-optical devices.

In the first part of this presentation, the principle of microwave filtering using optical interferometers is described for both optical coherent and non-coherent regimes. Optical components are addressed in terms of microwave-optical S parameters. The experimental realization of filters using fibers or integrated optics is explained.

In the second part, the use of optoelectronic techniques to control microwave devices is presented. For example, optically controlled switches and phase shifters can be useful for phased array antennas. Applications can be found also in the generation of millimeterwaves, optical probing, new microwave wide band devices ...

1- INTRODUCTION

Processing microwave signals on the optical link, directly in the optical domain, avoids intermediate conversions from optics to electronics (O/E) and then back again from electronics to optics (E/O). New functions are generated at microwave frequencies by processing the RF modulating signal of the optical carrier.

By using ordinary low-cost passive optical components like interferometers, some interesting microwave functions can be generated. For example, the interference of the microwave envelope and the optical carrier generate filtering of the microwave subcarriers. Microwave filtering obtained with this method is not frequency limited unlike in the microwave domain : filtering is periodic, and extends to infinite frequency. It can be achieved in the optical domain with low cost and low-loss components. Consequently, it is interesting to process filtering optically functions at higher frequency, where it is not easily realized in the microwave domain.

1.1. All optical processing of microwave functions by insertion of an optical passive component

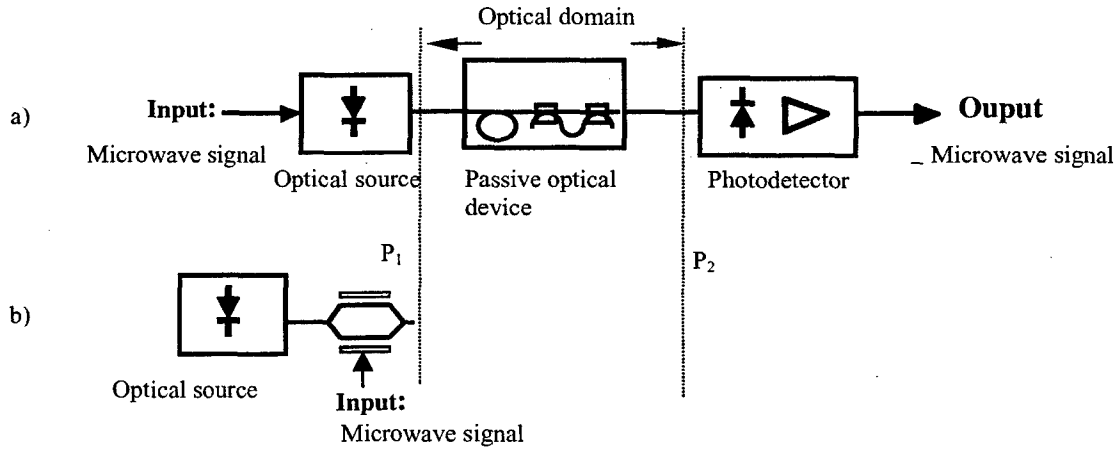

Figure 1: Insertion of optical components in the microwave link for all-optical signal processing.

In Fig. 1 is shown the point to point optical link with direct modulation (Fig. 1a), or external modulation (for example, electro-optical modulation using a Mach Zehnder interferometer, Fig. 1b). Optical passive

Paper presented at the RTO SET Lecture Series on "Optics Microwave Interactions", held in Jouy en Josas, France, 2-3 September 2002; Duisburg, Germany, 5-6 September 2002; Budapest, Hungary, 9-10 September 2002, and published in RTO-EN-028.

devices can be inserted between planes P_1 and P_2 for achieving optical processing of the microwave subcarrier. A passive interferometer inserted there, and made either of fibers and couplers or integrated optical waveguides, can realize microwave filtering. This solution is presented in section 2. In section 1.2, we discuss the transfer function of the filter in terms of S parameters and their variations with frequency.

1.2. Measurement of the optoelectronic scattering parameters

We consider here the external modulation, where the optical intensity is modulated at a microwave frequency (modulation index m).

It is convenient to define the optoelectronic S parameters as in microwave. The optical scattering waves (a_i, b_i) at each port, i , of the optical device, related to modulated optical intensity (envelope of the carrier) are :

$a_i = I_{ai} m \cos(\omega_m t + \varphi_{ai})$ and $b_j = I_{bj} m \cos(\omega_m t + \varphi_{bj})$, where φ_{ai} is the phase of the microwave envelope at port i, related to the incident wave a, and φ_{bj} relates to the emergent wave b. I_{ai} is the incident optical intensity at port i, I_{bi} the emergent optical intensity at this port.

The optoelectronic S parameters of the optical device can then be defined as :

$$S_{ij,opt} = \frac{b_i}{a_j} = \frac{I_{bi}}{I_{aj}} \exp j(\varphi_{bi} - \varphi_{aj}). \qquad (1)$$

These S parameters defined with the optical intensity can be measured with a microwave Vector Network Analyzer and its lightwave extension (Fig. 2).

The intensity of the light emitted by a DFB laser source (1300 nm) is modulated at the microwave frequency f_m by a microwave source modulating a MZ external modulator (E/O conversion). At the output of a rapid photodetector (O/E conversion), a synchronous detection is operated by the Vector Network Analyzer. The photocurrent detected by the photodetector is compared to a reference signal. The optoelectronic S parameters are then obtained. The microwave frequency response, the insertion loss, the group delay, etc. are finally derived.

Assuming a linear operation of E/O and O/E converters, then the optoelectronic transfer function $S_{21,opt}(f_m)$ of the optical device in the planes P1-P2 can be obtained by measurements. A preliminary calibration is done, then the E/O and O/E are extracted. The global transfer function T_{global} is then measured in the reference planes P3-P4 and then, the final transfer function requested in the reference planes P1-P2 is finally derived :

$$S_{21,opt}(f_m) = \frac{T_{global}(f_m)}{T_{E/O}(f_m).T_{O/E}(f_m)}. \qquad (2)$$

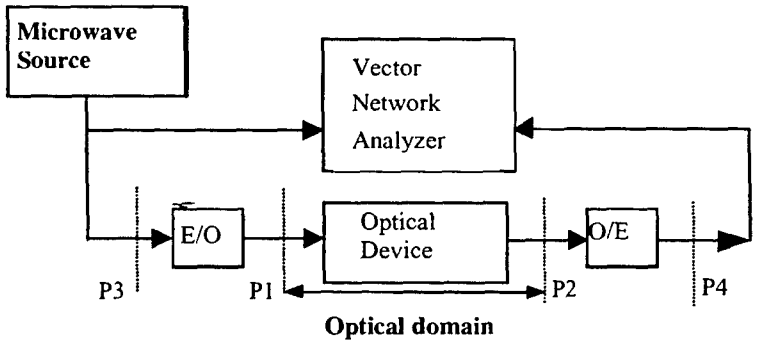

Figure 2: Measurement of optoelectronic S parameters

2- GENERATION OF MICROWAVE FILTERING

The solution presented here is based on interference (coherent regime and incoherent regime) using a directly modulated distributed feedback laser diode (DFB LD) and a passive unbalanced Mach-Zehnder (UMZ) interferometer [1]. Other solution has been presented that uses cascaded passive Mach-Zehnder (UMZ) interferometers [2].

The microwave filter consists of a single optical unbalanced Mach-Zehnder interferometer, which is composed of two optical directional 3dB-couplers separated by two unequal optical paths L_1 and L_2, when

fibers are used (Fig. 3a). It can also be realized in integrated optics on glass, with two Y junctions separated by two optical integrated waveguides of different lengths : one straight, the other curved (Fig. 3b).

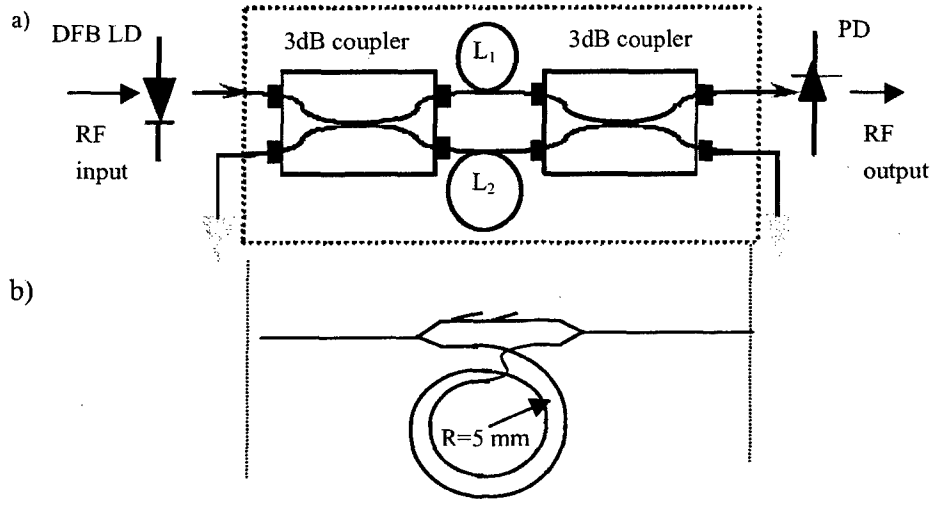

Figure 3 : UMZ: Unbalanced Mach-Zehnder used as a microwave filter made of a) fibers b) integrated optical waveguides on glass

Because of the path difference $\Delta L = L_2 - L_1$ between the arms of the UMZ interferometer, two interference figures can occur at the output of the interferometer :

- microwave interference on the envelope - This occurs when two non-coherent optical pulses arrive at the same time at the output of the UMZ. This is the case when the coherent length Lc of the source is shorter than ΔL. The intensity at the output is the sum of optical intensity $I_1 + I_2$ on each arm.
- microwave interference on the envelope plus optical interference on the optical carrier - This occurs when the laser coherence length is greater than the path difference, $Lc > \Delta L$.

In each case, the RF frequency period of the transfer function $S_{21}(f_m)$ equals the FSR (Free Spectral Range) of the interferometer, which is defined as :

$$\frac{n_{eff}}{c}(L_2 - L_1) = \frac{1}{FSR} = \tau. \qquad (3)$$

The optical intensity at the output of the UMZ interferometer is

$$I(t) = I_1(t) + I_2(t-\tau) + 2\sqrt{I_1(t).I_2(t-\tau)}\cos(\Omega_0\tau).V(\tau). \qquad (4)$$

Loss of coherence in the two waves propagated on the two arms of the interferometer is illustrated by $V(\tau)$, which equals 0 in incoherent regime and is approximately 1 in the coherent regime

2.1. Non-coherent regime

The interference of the modulated intensity waves in the two arms produces a periodic transfer function $S_{21}(f_m)$ with minima and maxima. The microwave frequency of the minima is an odd integer multiple of FSR/2, that of maxima is an integer multiple of FSR.

The UMZ acts as a frequency rejection filter over a large frequency range. Filtering is periodic, period equals FSR that can be set by adjusting ΔL. A rejection ratio (maximum divided by minimum of $|S_{21}|$) greater than 50 dB electrical (25 dB optical) can be obtained.

It is worth noting that such a similar value for the rejection ratio could not be obtained in the microwave range, and moreover periodically, up to infinite frequencies if there were no limitation in the frequency response of the optoelectronic components at emission and detection sides.

2.2. Coherent regime

This regime exists when the coherence length of the source is high enough to be greater than ΔL. The coherent optical interference suffers from some additional effects :

a) influence of the optical phase of each arm and influence of the refraction index. The temperature of the component must be controlled accurately;
b) influence of the linewidth of the laser, and of the wavelength emitted (by accurate control of the DC bias and temperature of the LD);
c) influence of polarization of the light, when the optical waveguides used in the UMZ are birefringent.

2.3. Experimental results with passive UMZ interferometer integrated on glass

The example of a passive optical UMZ interferometer integrated on glass substrate by Tl+/Na+ ion exchange is presented here. The design allows a FSR of 3 GHz (ΔL=6.3 cm). The layout of the UMZ is shown in Fig. 4a, and is similar to the schematic of Fig. 3b. In the coherent regime of interference, a DFB laser diode source emitting at 1300 nm (coherence length ≈ 5m) and modulated by an external modulator (20 GHz of bandwidth is used. The optoelectronic transfer function $S_{21}(f_m)$ can be obtained, as shown in Fig. 4b.

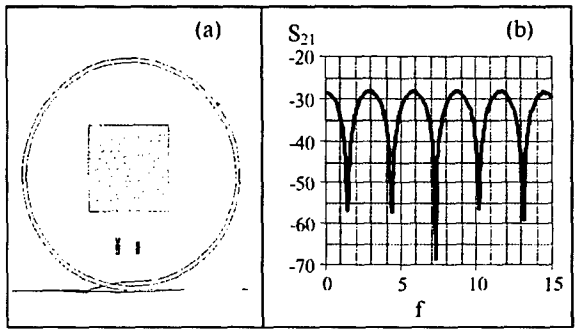

Figure 4 : layout of the integrated UMZ (a) and the corresponding measured frequency response (b).

This figure exhibits deep frequency rejections, periodical, at frequencies equal to an odd integer multiple of FSR/2 as explained before. The path difference ΔL can be adjusted (thermo or piezzo-electrical control) to have a rejection at the desired frequencies.

3. INTEGRATED OPTICALLY CONTROLLED PHASE SHIFTER

In phased array antennas, control of phase of RF signals is of major importance. Optical fibers or optical waveguides are used to distribute the control signal and offer gain of weight, of power consumption and of cost in comparison with electronic control. Thus, the introduction of these optical devices into microwave systems is very important for aircraft radar systems or in satellite communication systems where optical control of microwave devices can be applied for signal processing. A phase shifter and a microwave switch are described here. The monolithic integration of the optical waveguide offers the flexibility and precision of the optical guiding for illumination of the semiconductor device and avoids the presence of multiple beams for controlling different cells of the array.

Microwave circuits are here integrated on silicon, and their responses are modified under illumination. In the semiconductor, the light produced by a laser emitting at a wavelength in the visible range (λ=514 nm) or in the near infrared region (λ=840 nm) is absorbed, then charge carriers are generated, thus modifying the local conductivity of the semiconductor. Silicon has the advantage over GaAs to offer large carrier lifetime and important diffusion lengths. As a consequence, large variation in the conductivity of the semiconductor can be obtained for moderate illumination powers.

The optical microwave planar devices are either integrated on high resistive silicon substrate with a fiber illumination on top of the device, or they are monolithically integrated on a SOI (Silicon on Insulator) structure. In the latter case, the optical guide that illuminates the device is embedded in the structure, thus enabling a large flexibility to position the illumination wherever needed in the circuit. The novelty of this solution is that the monolithic integration results in a mixture of MMIC (monolithic microwave integrated

circuits) and OEIC (optoelectronic integrated circuits). The silicon technology chosen offers a large maturity and allows a high integration level while the SOI technology (used here for monolithic integration) is very promising for microwave applications, because of the low propagation loss. The optically passive controlled devices can be further co-integrated with MMIC on silicon, to realize sub-systems like optically controlled VCO, amplifiers...

3.1. Optical controlled microwave switch on bulk silicon

Here a high resistive (5000 Ω.cm) is used and aluminum coplanar lines are etched on top of it.

The gap (see Fig. 6) inserted in the signal line acts as a microwave phase shifter and as a switch, both controlled by the light emitted by a laser diode ($\lambda = 840$ nm). Note that here, only a bulk silicon substrate is used and illumination is made on top of the cell. The gap size is of the order of 16µmX100 µm. After on-wafer calibration, S parameters have been measured for both dark ("off") and illuminated ("on") states.
The variations of S_{21} with frequency are shown in Fig. 5 in the "off" and "on" state.

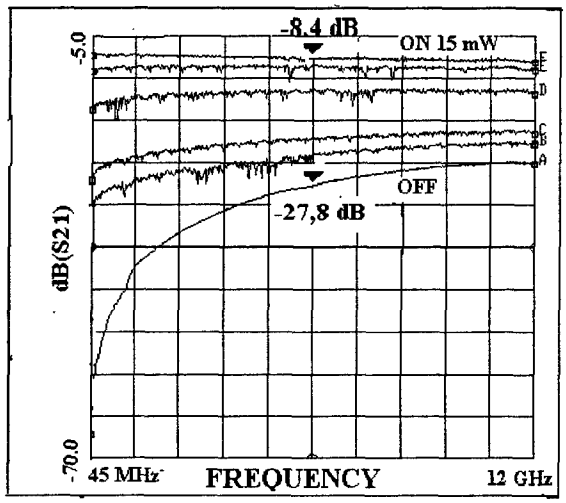

Figure 5 : S_{21}(f) for the microwave switch on bulk silicon

A large on/off ratio can be obtained; the value is 20 dB around 6 GHz with 15mW of optical power, and the insertion loss is around 8 dB.

3.2. Optically controlled switch integrated on a SOI type structure

Here, we discuss optical integration of the illuminating waveguide.

Guided wave optics based on Silicon-On-Insulator have gained interest since they offer low cost and well established technology [3] and they are compatible with monolithic microwave integrated circuits in CMOS and BiCMOS technology that works now in the GHz range. The etched buried channel optical waveguide used here and realized in this technology has been fabricated at CEA/LETI in Grenoble [4] and the fabrication procedure has been given in details in Ref. [5-6]. In the final integrated structure of Fig. 6, the polysilicon gap inserted in the signal strip of a coplanar waveguide is optically controlled by the monolithically integrated optical waveguide embedded in the SOI structure. Here, two illuminating conditions are compared : top fiber illumination with optical power of 2.4 mW and integrated illumination with optical power of 2 mW. It can be concluded from Fig. 7 that the same switching performances can be observed whatever the way of illumination is.

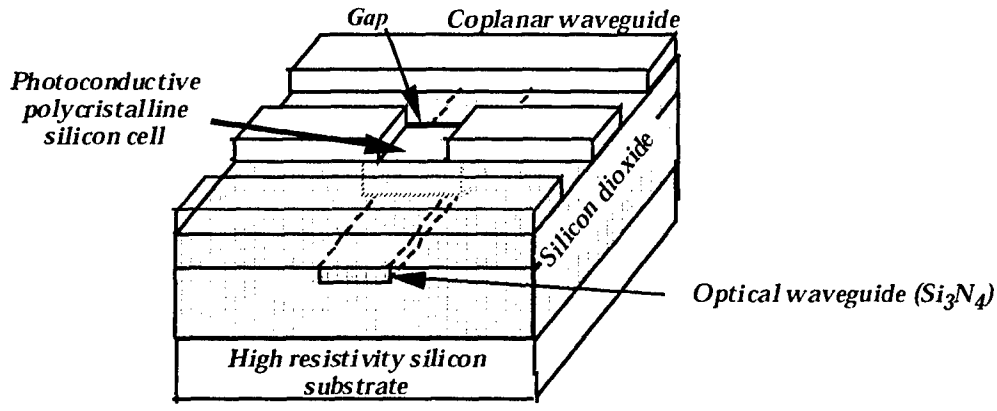

Figure 6 : Schematic view of the optical/microwave device.

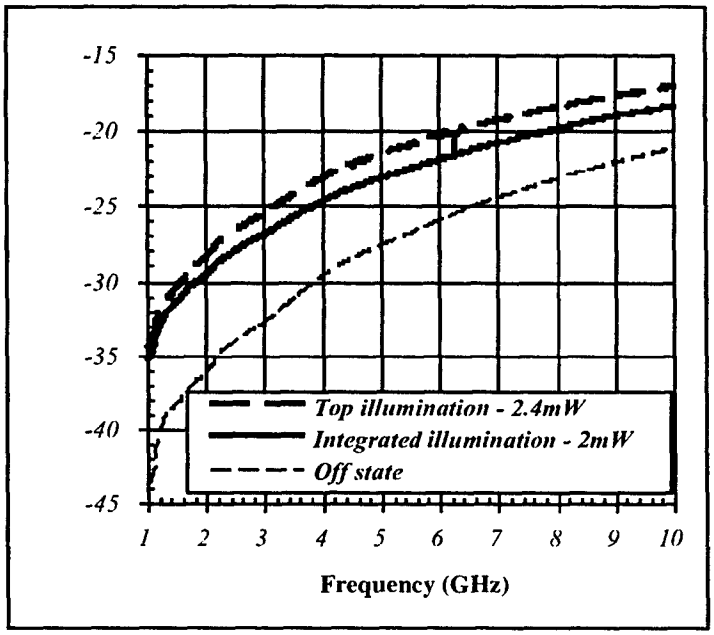

Figure 7 : Comparison of switching performances under 2mW of optical power for the full integrated structure on SOI and 2.4 mW of optical power with top illumination.

3.3. Phase shifter performances in a bulk Si structure

In the monolithic integrated device shown previously, deposited polysilicon has been used for the gap since wafer bonding (monosilicon) is difficult to realize. The performances reached with undoped silicon are better than with polysilicon because of larger values of the diffusion length and of carriers lifetime. But a compromise must be chosen between optical control efficiency and faster response of the device. In this section are discussed the performances of the phase shifter realized in bulk silicon with top illumination, having in mind that top and integrated illumination would lead to the same results as explained in the previous section. Fig. 8 shows the phase shift of S_{21}, under dark and illumination. It reaches the value of 76° at 1.4 GHz and 56° at 12 GHz for an illumination power as low as 5 mW.

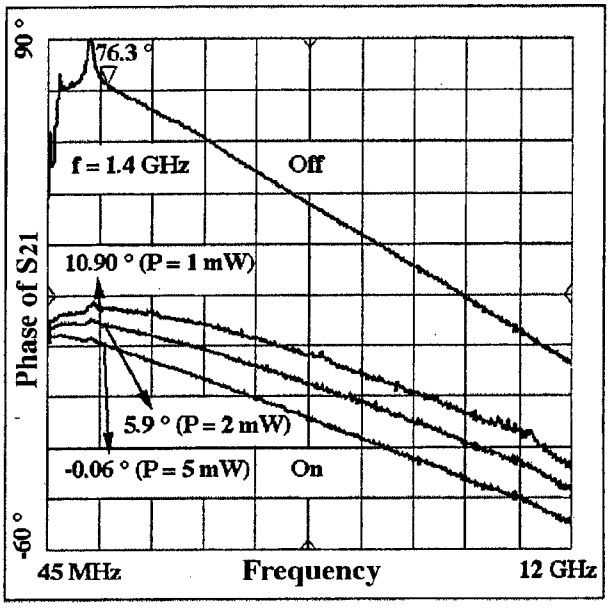

Figure 8 : Phase of S_{21} as a function of frequency in the "off" state and the "on" state for an optical power of 1, 2 and 5 mW.

3.4. Model of the phase shifter

The electron-hole plasma created in the semiconductor results in modifications of conductive as well as dielectric properties of the device. In polysilicon, these effects are limited to a thin layer near the illuminated surface, while in bulk silicon these effects are widely distributed in the substrate. Consequently, the effects observed in the illuminated gap can be modeled by an equivalent circuit composed of a Π network of series connected cells (see Fig. 9), each cell made of shunt connected resistor and capacitor. In this way, the frequency dependence of the gap response (transmission and reflection) is considered together with the modifications of the response under illumination and the distributed effects in the substrate thickness.

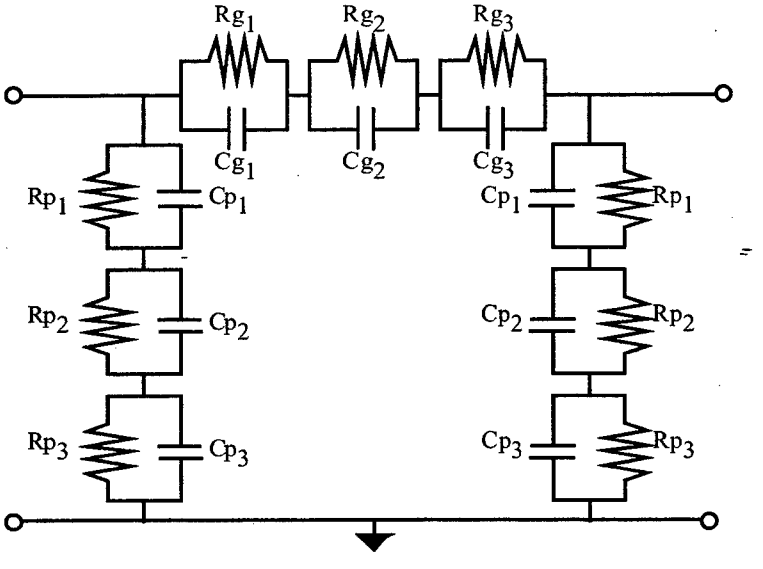

Figure 9 : Equivalent circuit of the gap.

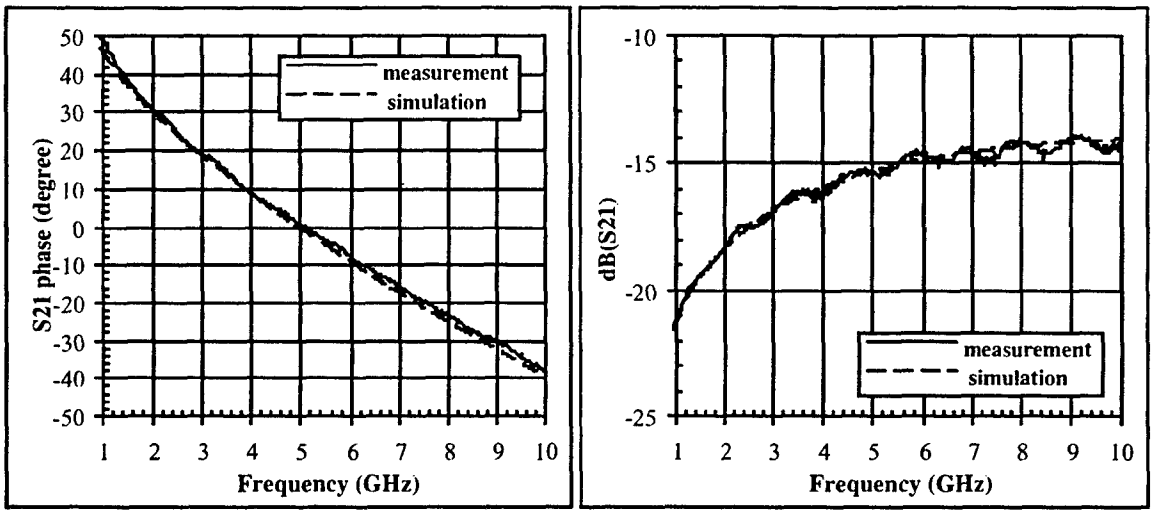

Figure 10 : S21 magnitude and phase variations – Comparison between simulation and experimental results related to the "on" state.

ON state		OFF state	
Rp_1 (Ohms)=160	Cp_1(fF)=1190	Rp_1 (Ohms) $>10^8$	Cp_1(fF)=10^{-3}
Rp_2 (Ohms)=10^5	Cp_2(fF)=3370	Rp_2 (Ohms) $>10^8$	Cp_2(fF)=2.5
Rp_3 (Ohms)=130	Cp_3(fF)=25	Rp_3 (Ohms) $>10^8$	Cp_3(fF)=0
Rg_1 (Ohms)=3.10^5	Cg_1(fF)=845	Rg_1 (Ohms)=3.10^5	Cg_1(fF)=103
Rg_2 (Ohms)=3.10^5	Cg_2(fF)=829	Rg_2 (Ohms)=5.10^5	Cg_2(fF)=23
Rg_3 (Ohms)= 3.10^5	Cg_3(fF)=1109	Rg_3 (Ohms)=5.10^5	Cg_3(fF)=25

Table 1 : R and C values under dark and illumination for the optically controlled phase shifter on silicon.

Simulations of the equivalent circuit related to the optically phase shifter on silicon have been carried out using Advanced Design System software (ADS) from Agilent Technologies. From Fig. 10, it can be seen that the modeled S_{21} phase and magnitude values are in very good agreement with experimental results. The values of modeled capacitances and resistances under dark and illumination are indicated in Table 1. It can be concluded that both capacitances and resistances exhibit a great variation under illumination.

4- CONCLUSIONS

It has been demonstrated that microwave functions can be generated with all optical components. Photonics-microwave rejection filters with high extinction ratio, not limited in frequency range, have been presented. They use a passive unbalanced Mach-Zehnder interferometer, low loss and low cost.

Optical control of a microwave switch and phase shifter has been presented. The phase shift of 76° has been confirmed in a silicon gap structure under an optical power as low as 5 mW. The optical control avoids physical connection to the circuit and avoid biasing components that are usually used in electrical switches. These optically controlled systems are advantageous for wide-band signal transmission and produce novel microwave systems of enhanced capabilities. They can also be applicable to fiber optic fed microwave systems such as phased array antennas.

References

[1] An Ho Quoc, "Etude et Réalisation de Dispositifs Tout-Optiques pour le Traitement de Signaux Rapide", PhD thesis, INPG Grenoble, France, July 1996.
[2] T.A. Cusik, S. Iezekiel, R.E. Miles, S. Sales, J. Capmany, "*Synthesis of All Optical Microwave Filters Using Mach Zehnder Lattices*", IEEE Trans. on Microwave Theory Tech., vol. MTT-45, pp. 1458-1461, August 1997.
[3] U. Hilleringmann and K. Goser, "*Optoelectronic System Integration on Silicon, Photodetectors and VLSI CMOS Circuits on One Chip*", IEEE Trans. Electron Devices, vol. 42, pp. 841-845, 1995.
[4] P. Mottier, "*Integrated Optics at LETI*", International Journal of Optoelectronics, Vol. 9, Nr 2, pp. 125-134, 1994.
[5] S. Chouteau, B. Cabon and J. Boussey "*Integrated Optics on Silicon substrate for Microwave Applications*", 28 th European Microwave Conference, Amsterdam 6-8 October 1998, Proc. pp. 70-74.
[6] S. Chouteau, J. Boussey, B. Cabon, A. Illiadis, "*Optoelectronic Microswitch on SOI Based Structure*", IEEE International SOI Conference, 1995, Proc. pp. 40-41.